ELSEVIER

Tectonophysics 337 (2001) 191–208

TECTONOPHYSICS

www.elsevier.com/locate/tecto

Forward and inverse modelling of gravity revealing insight into crustal structures of the Eastern Alps

J. Ebbing[a], C. Braitenberg[b], H.-J. Götze[a,*]

[a]*Institut für Geologische Wissenschaften, FR Geophysik, Freie Universität Berlin, Malteserstrasse 74-100, D-12249 Berlin, Germany*
[b]*Dipartimento di Scienze della Terra, Università di Trieste, Via Weiss 1, 34100 Trieste, Italy*

Received 15 December 2000; accepted 11 May 2001

Abstract

The crustal structure of the Eastern Alps is less known than that of the Western Alps as participants of the European Geotraverse and particular Swiss projects investigated the Alpine crust there. Recently, the Eastern Alps were subject to seismic research which was conducted in the context of the German, Austrian and Italian TRANSALP project. The 3D modelling of the density structure which is presented in this paper belonged to a series of piggy-back projects which were closely accomplished using the seismic reflection studies. We present a combined gravity–seismic interpretation which is based on the results of both older deep seismic profiles, and the new TRANSALP profile. Special emphasis was laid on geologic and tectonic information which served as model constraints for near-surface structures. A 3D forward modelling of both the Bouguer gravity field and the geoidal undulations provides in-depth insight into the lithosphere and considers the constraints. Due to the uncertainties of used constraints, particularly in depths of the Eastern Alpine Moho, an inversion technique complemented this study and provided insight into the shape and density contrast at the crust–mantle interface.

The modelling indicates that the Bouguer gravity field in the Eastern Alps is mainly caused by two sources: the density contrast at the crust–mantle boundary (350 kg/m^3) and the density inhomogeneities in the upper 10 km of the crust, which contributes to the overall gravity field by amounts of approximately 30×10^{-5} m/s^2. The results of the forward and inverse modelling produced a shallower crust–mantle boundary in the (southern) Adriatic area in comparison with the northern part, and differs from the seismic findings of the TRANSALP group to some extent. This observation and observable mismatch in the long wavelength model and the observed geoidal undulations point to density inhomogeneities in sub-crustal and even sub-lithospheric depths. These deep seated inhomogeneities should have a substantial bearing on the isostatic balance of the Eastern Alps.

Keywords: Eastern Alps; collision belt; crustal structure; gravity; forward modelling

1. Introduction

In recent years renewed interest has been shown to the understanding of the structure of the Eastern Alps due to the efforts of the multidisciplinary TRANSALP research project. The TRANSALP-Traverse extends from Freising (D) in the north to Treviso (I) in the south and is carried out by the TRANSALP working group, with members from Italy, Austria, Switzerland and Germany. During 1998 and 1999 a seismic reflection profile was investigated over a length of 340 km, covering the Eastern Alps and parts of the northern

* Corresponding author. Tel.: +49-30-83870874; fax: +49-30-7753078.
E-mail address: hajo@geophysik.fu-berlin.de (H.-J. Götze).

0040-1951/01/$ - see front matter
PII: S0040-1951(01)00119-6

and southern molasse basins. The new results, stemming from the seismic profile and from the numerous interdisciplinary projects that accompany the seismic survey, make a new 3D gravity modelling necessary.

Previous gravity investigations of the Eastern Alps have been made using the interpretations of seismic lines shot in the sixties and seventies (e.g. Makris, 1971; Mueller and Talwani, 1971; Schöler, 1976; Wagini et al., 1988) and more recently, by using revisions of all available profiles (Dal Moro et al., 1998; Cassinis et al., 1997; Braitenberg et al., 1997). The investigations of the Eastern Alps will be a good supplement to the knowledge of the Western Alps, which have also been intensively studied due to the effort of the European Geotraverse and the Swiss project NRP 20 (e.g. Pfiffner et al., 1997). In the field of gravity investigations we refer to the works of Klingelé et al. (1990), Schwendener (1990), Schwendener and Mueller (1990), and Holliger and Kissling (1992).

The lower crustal structure of the Eastern Alps is a rather controversial problem, above all the geometry of the crust–mantle boundary remains unclear and in a sense speculative. This discomforting situation resulted in conversations which led to the realization of the TRANSALP consortium and the observations along the reflection profile.

Mainly two different hypotheses have been discussed. Miller et al. (1977) proposed a lithospheric velocity model of the Eastern Alps, which features a more or less gentle and continuous crust–mantle boundary at the transition zone of the Adriatic and European domain. In contrast, Giese et al. (1982) proposed crustal doubling in the area of the Afro-European transition zone. In this last interpretation, the Adriatic plate overrides the European plate, leading to an interference of the two crusts and crustal doubling at the transition zone. In recent years, the revision of the available DSS data (Rosner, 1994; Scarascia and Cassinis, 1997) produced modified lithospheric velocity models in favour of this last hypothesis. One of the problems addressed by the TRANSALP research group, was the investigation of orogenic processes driven by the collision of continental lithospheric plates in the area of the Eastern Alps. Structures and orogenic processes of the Eastern Alps are considered paradigmatic for testing plate-tectonic models of continent–continent collision by reflection seismic methods (e.g. Lueschen and TRANSALP Working Group, 2000). The new image of the crust, e.g. by near vertical reflections and other seismic experiments also fosters interdisciplinary interpretations by different disciplines through reduction of ambiguity which was typical in the former studies.

As a new procedure we intend in the present study to investigate the lithospheric density structure, by matching both the observed gravity fields and the geoidal undulations. In this connection, we employ constraining information from newly published results of the TRANSALP group (Lueschen and TRANSALP Working Group, 2000) and combine direct 3D forward modelling with inversion tools for Bouguer gravity interpretation. In our study the 3D forward modelling of near surface structures in the upper 10 km of the crust, provides an interpretation of short wavelengths and combines reflection seismic data with geological models, cross sections and surface observations. In contrast, one should reckon with greater ambiguities the velocity distribution and geometry of crustal domains which are based on seismic surveys of the lower crust, e.g. the TRANSALP survey did not reveal the depth of the Moho along the profile due to technical problems along the central section of the profile which is superimposed by strong effects of crustal anisotropy.

Bearing these uncertainties of seismic results in mind, the density modelling of the lower crust was done by two different techniques in this study, which considers deep seismic results as soft constraints. Both, forward modelling by the aid of an interoperable geoinformation system (IOGIS) and inversion of the crust–mantle interface essentially lead to a rather similar geometry of the Moho undulations. Firstly, 3D modelling of the lower crustal parts was supported by blending all available geometry and velocity information with the density model by the aid of the 3D information system. From this we constructed the initial model which based its deeper parts on pre-existing Moho models. In the course of the modelling process this starting density model was interactively modified in order to match the observed Bouguer gravity. The second approach used a gravity inversion technique, applied to a Bouguer gravity field from which the gravity effects of upper crustal

structures were stripped off. This approach is restricted to modelling the Moho undulations only.

2. Geological setting

The Alps are an orogenic belt extending from the French-Mediterranean area to Switzerland and Austria. The present geologic structure can be understood as a result of tectonic processes, which include both extensional and compressional strain regimes, subduction of oceanic crust and collision of continental blocks due to plate motions (Frisch, 1979). In the following the evolution of Alpine orogeny will be described briefly.

In the late Palaeozoic, the Pangea continent was built by the Variscan orogeny, partly overlain by the shelf area of the Tethys ocean bordering in the SE. Three main regions of sedimentation can be distinguished from north to south: the Helvetic, Penninic and Austroalpine realm. In the early Jurassic, the southern Penninic ocean was created due to the opening of the Pangea continent, isolating the Austroalpine realm. Between the Helvetic and the Penninic zones, a further relatively small basin developed in the lower Cretaceous creating the small Middle Penninic continent, while in the south subduction of the southern Penninic oceanic crust began. During Mid-Cretaceous the collision process began with an overthrust of Austroalpine units onto Penninic.

Compression continued up to the lower Tertiary, when the northern Penninic ocean was closed and the nappe structure was overthrusted to the north onto the European continental margin, accompanied by folding and faulting of the rocks into thrust sheets. These movements stopped during Quaternary ages. The resulting pronounced nappe tectonics of the Eastern Alps is shown in Fig. 1 (after Berthelsen et al., 1992). In the so-called Tauern window the Penninic base was uncovered by cutting the overlying Austroalpine nappes due to erosion and tectonic uplift processes. The molasse zone in the north of the Alps consists of sediments in a deep geosyncline in front of the nappe pile and is overthrusted. This is supported by deep borehole drillings within the northern Calcareous Alps. To the south of the Alps, in the Po basin, a foredeep evolved where syntectonic sediments could accumulate, linked to south vergent thrusting in the Southern Alps (Roure et al., 1990). Besides, some rocks of magmatic/plutonic origin occur at the Po-Basin–Dolomites transition.

This leads to the modern Alps as imaged today and we seek to use these principal geological domains for modelling in case they differ significantly in densities. The density model, which we present, includes most of the tectonic units (for density values, refer to Chapter 4) and their geometrical structure as implied by tectonic history. This is necessary to fit small-scale anomalies of the modelled and measured field. In particular, uplift masses of the Tauern window and eroded masses of the Penninic and Helvetic nappes are important components of the density model of the Eastern Alps which cause the observed gravity field. In the next part we will describe the geophysical data set which was used, together with the tectonic information which were defined in this paper.

3. Geophysical database

3.1. Bouguer anomaly

The Bouguer gravity field used for modelling purposes was taken from three different gravity data sets. The northern part Germany is covered by ~5500 points, released by the GGA (Hannover), the Austrian central part by ~3700 sites (B. Meurers, University of Vienna), and the Italian southern part and the Adriatic Sea by ~3800 data points by the Bureau Gravimetrique International (BGI, Toulouse), which is thankfully acknowledged.

The density for the station complete Bouguer reduction was 2670 kg/m^3 for all continental masses and 1030 kg/m^3 for the water in the Mediterranean Sea. The data sets were subsequently homogenized, that is they were linked to the IGSN71 gravity datum, terrain reduced with approximation of topographic masses by polyhedrons within a radius of 200 km (Müller, 1999; Götze and Lahmeyer, 1988). The mean elevation corresponds to the heights of the observation points. Data errors were assumed to be less than 2×10^{-5} m/s^2 (2 mGal), in general, for the land data and less than 5×10^{-5} m/s^2 for the offshore area of the Adriatic Sea.

The topographic data (Fig. 2) used for reduction are based on the GTOPO30 data (US Geological Survey,

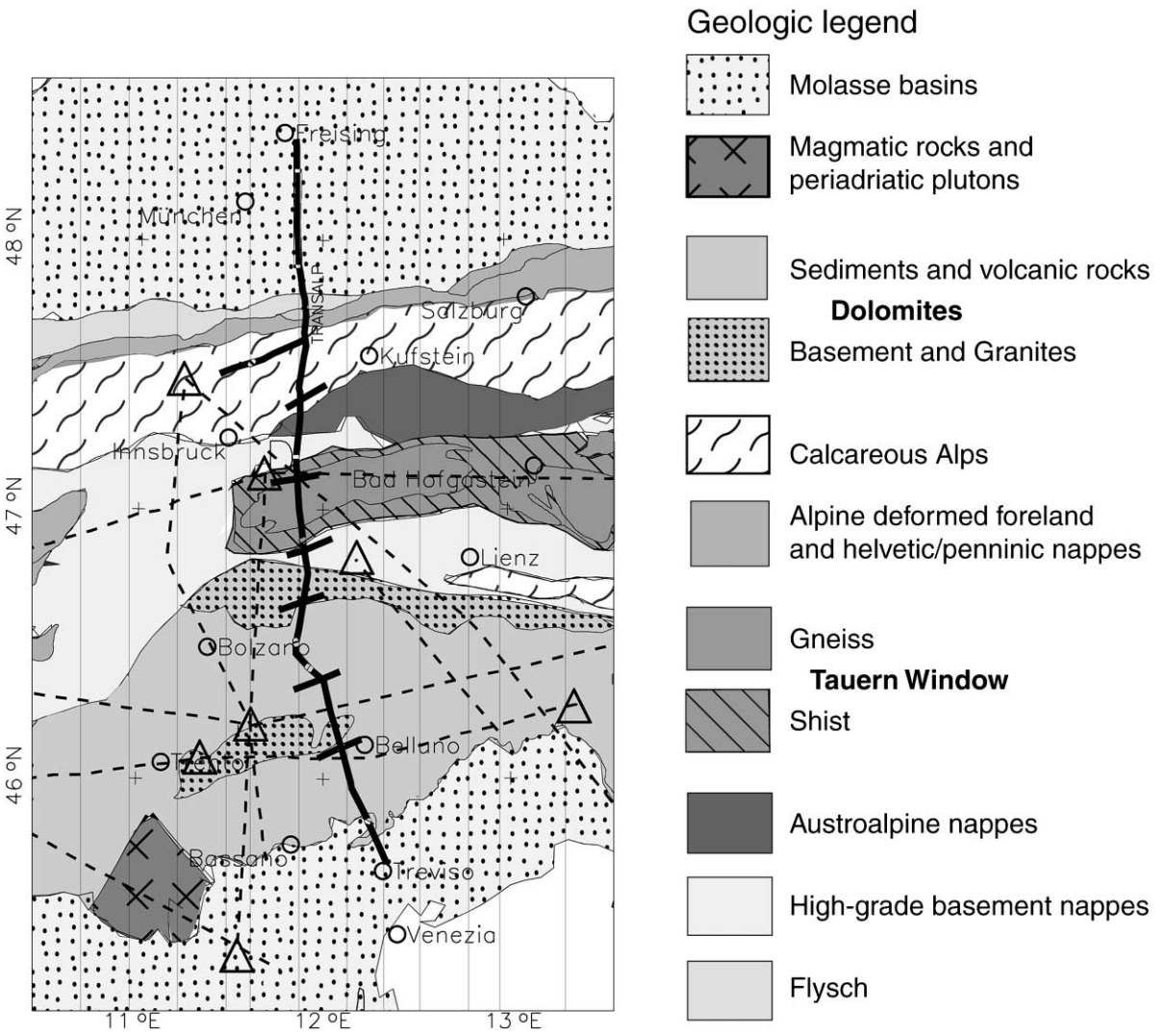

Fig. 1. Sketch map of major geological divisions along the TRANSALP-Traverse (after Berthelsen et al., 1992). The solid N–S lines show the position of vertical cross-sections of the density model. The thick black lines present the position of the TRANSALP seismic lines and the dotted lines the main DSS profiles available in the Eastern Alps (after Scarascia and Cassinis, 1997), which were used to construct the initial density model.

2000) with additional data for offshore areas by Sandwell et al. (2000).

The Bouguer anomaly field in Fig. 3a is based on these homogenized data sets. The observed low maximum gravity in the area of the central Alps accounts for -220×10^{-5} m/s^2, which is simultaneously the most low distinct gravity in the central Europe. A relatively smooth and regular gradient is observed in the north, dipping south towards the axial zone and contrasting with the steeper and more irregular gradient observed in the southern area, thus suggesting an asymmetrical crustal lithospheric structure. A pronounced low in the east of the region correlates with the position of Helvetic and Penninic nappes, and continues to the west into the area of the Tauern window and appears to be much narrower and elongated, thus suggesting a different structure in both shallow and deep crust. In the southwestern

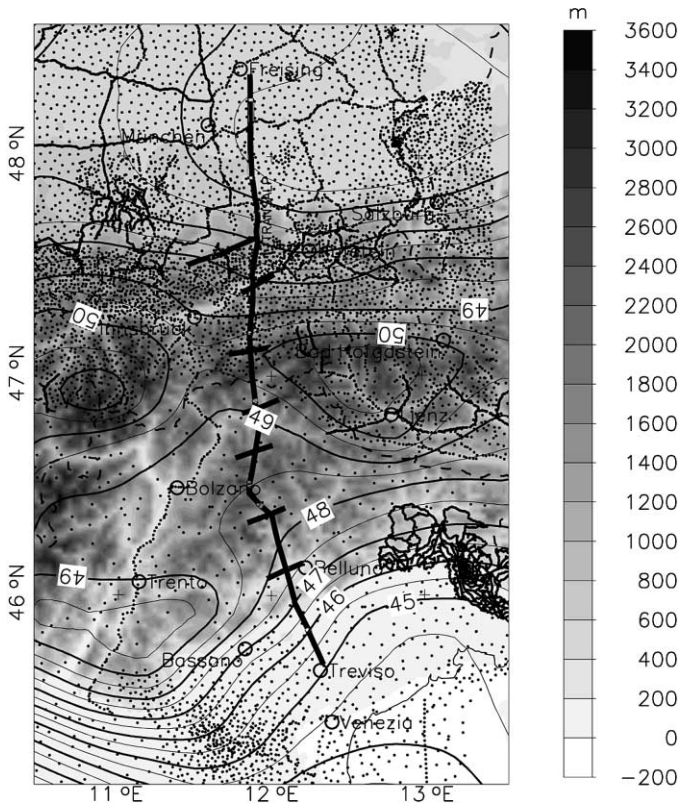

Fig. 2. Greyscale presentation of Alpine topography along the TRANSALP transect overlain by contours of geoidal undulations (redrawn after Lelgemann and Kuckuck, 1992). Contour line intervals are 1 m. The dots represent measured stations of the gravity field.

part of the area a high gravity is observed, generated by both crustal thinning and the presence of plutonic rocks.

3.2. Geoidal undulations

To complement the modelling of shorter and middle wavelengths by matching the Bouguer anomaly field we focussed on geoidal undulation to model long wavelengths in the gravity field. These data were published in the EGT-atlas by Lelgemann and Kuckuck (1992). Primarily the geoid data were computed at a grid size of $12' \times 20'$ with an accuracy of $\sim$1 m. A first glance (Fig. 2) reveals the relatively smooth gradient in the north, two separated areas with maximum values in the central part of the orogene, and a relatively steep gradient to the south. A preliminary correlation of the geoidal undulations with the topography results in a slightly phase shifted position of the compared fields, which indicates long wavelength sources in the lithosphere.

The geoid data are affected by topography and density structures as well. For matching 'geoidal undulations' and the Bouguer anomaly within the same 3D density model, the effect of the topography on the geoid has to be subtracted first. This necessary topographic reduction has been done analogously to the reduction of measured gravity data which led to a station complete Bouguer anomaly.

We calculated the topographic effect by the IGMAS software which will be introduced in the next part of the paper. A reduction density of 2670 kg/m^3 was used for land masses and 1030 kg/m^3 for water within a reduction radius of 170 km (167 km = Hayford O_2). The resulting terrain reduced geoidal undulations are shown in Fig. 3b.

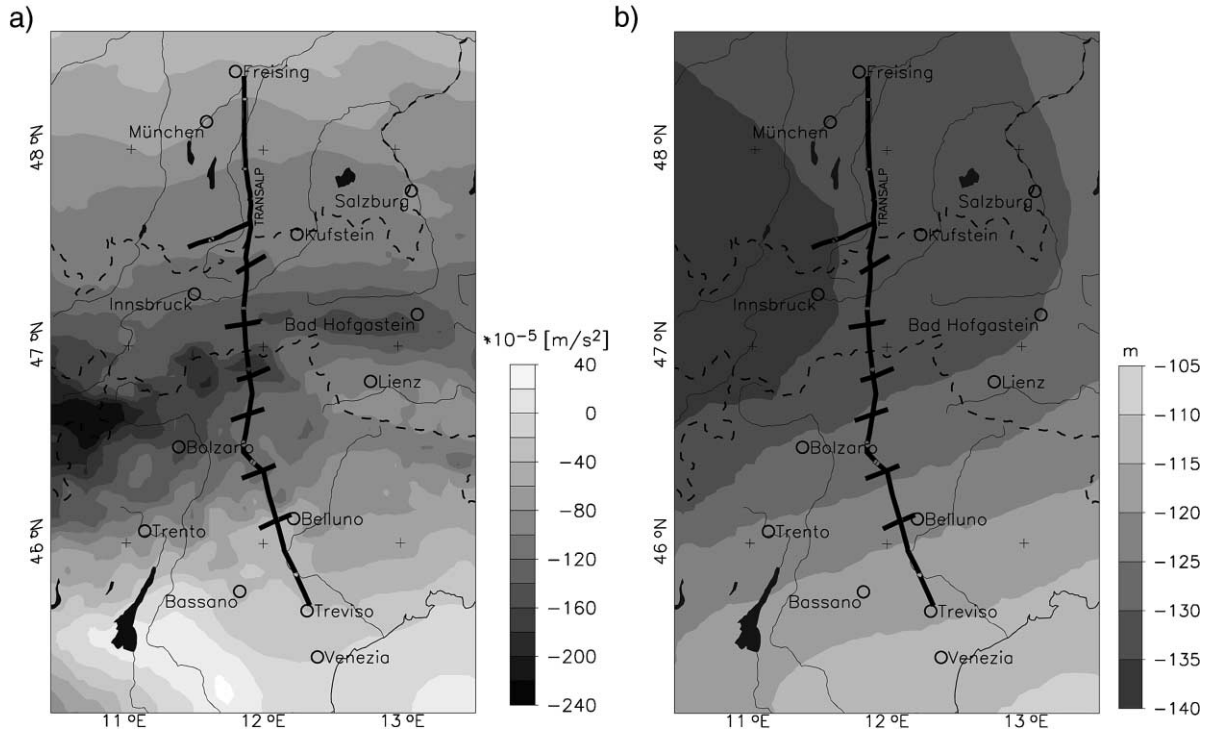

Fig. 3. Greyscale maps of the (a) station completed Bouguer anomaly, and (b) terrain corrected geoidal undulations.

Compared with the geoidal undulations the shape of the terrain reduced geoid amplifies density domains in the long-wavelength spectrum of the gravity potential. There is no obvious correlation to the topography, as expected, and the average value of the undulations is shifted from 50 m in the north to −130 m in the central part. The terrain corrected geoidal undulations show smooth gradients in the south, a minimum area in the central and north western (with up to −145 m) and in the northern part a west–east oriented gradient.

To compare the trend of the Bouguer anomaly with that of the terrain reduced geoid, one sustains that gravity is superimposed by different sources in different depths of the lithosphere. In comparison to the terrain reduced geoid, the alpine Bouguer field is characterized by variations of shorter wavelengths. Therefore, we have to match two independently 'observed' potential field data to modelled ones in different windows of spectrum. This will restrict model solutions and serve as additional constraint.

4. 3D forward modelling

The modelling software (e.g. Schmidt and Götze, 1998, 1999) employed in this study makes use of an interoperable 3D Geoinformations Systems (IOGIS) and its functionality. It enables the user to process as many available constraining data in the 3D space as possible, particularly from reflection and refraction seismic or near surface tectonics. However, other data and maps can be included into the IOGIS if they are available in a digital form, e.g. tectonic maps and information on sedimentary cover, as was done here.

Visualization tools were used to depict data and information from independent sources combined with model geometry and densities. For gravity modelling we used the interactive software IGMAS (math. background: Götze, 1984; Götze and Lahmeyer, 1988; Schmidt and Götze, 1998,1999; Breunig et al., 2000). All data sets mentioned here are available in digital form and can be used during the course of interactive modelling.

The study area covers the TRANSALP-Traverse and a 200-km-wide strip, 100 km to both east and west, along the traverse, covering a total area of 200 × 350 km (Fig. 1).

The 3D density modelling is made along 15 north–south-oriented parallel cross sections (Fig. 1). The spacing between the planes is ~10–30 km. These distances were used to ensure that the model approximates the size and location of the principal features of geological and geophysical bodies and domains well enough.

4.1. The reference model

Since Bouguer anomalies express only relative gravity data, density contrasts of all lateral inhomogeneities must cause the modelled field (La Fehr, 1991; Kirchner, 1997). Therefore and to avoid edge effects, a reference density model has to be considered for the use of absolute densities, which on top provides better opportunities to compare the density model with petrologic or seismic velocity models.

The used density model consists of a reference model for the background of our model. This reference model considers at least theoretically the layered density structure of a 'normal earth' and should result in the expression of the earth's 'normal gravity field', which is always subtracted from the absolute value of measured gravity while calculating Bouguer anomalies. In this study we used the IASPEI layered velocity model (Kennett and Engdahl, 1991), which was converted to a local reference density model by applying relations published by Christensen and Mooney (1995). The resulting reference model is divided into three layers: the upper crust (0–10 km: 2670 kg/m^3), the lower crust (10–32 km: 2900 kg/m^3) and the upper mantle (32–180 km: 3350 kg/m^3).

4.2. The 3D density model

The presented 3D density model consists of an upper part, where the results of the reflection seismic correspond to geologic models, and a lower part, where only seismic investigations provide constraining information on geometry and density. Long before the TRANSALP field work was conducted, seismic profiles were investigated in the Eastern Alps. Fig. 1 shows a series of most prominent seismic lines as from the 1970s, like ALP'75 (Alpine Explosion Seismology Group, 1976; Miller et al., 1982; Yan and Mechie, 1989), SudALP1977 (Italian Explosions Seismology Group, 1978, 1981; Deichmann et al., 1986), among others. All available data have been recently reprocessed by Scarascia and Cassinis (1997).

In a rather early state of density model compilation with the help of the available constraining seismic information we remarked differences between the reprocessed (older) seismic data base and the recently processed TRANSALP survey. Differences can be explained by different velocity models, and therefore, different density models which could not match the observed gravity field. Additionally, geometry of the velocity–density model domains differ and therefore cause differences. In these cases we followed mostly the seismic image which stems from recently done TRANSALP processing for the upper model layers, and a more or less free design in the deeper model parts which was guided by several surveys. However, we always tried to compromise the findings of former interpretations with the modern seismic data, where it was advisable; e.g. the completed velocity model 'Eschen-38' (Fig. 4) was used in this study as one of the main constraints for densities and geometric boundaries. This profile was modified and completed by the TRANSALP Working Group considering the new TRANSALP results (TRANSALP Working Group, 2001).

4.3. The upper 10 km of the crust

The densities of shallow geological bodies were taken from published data by Granser et al. (1989) and Schöler (1976). These density values are well constrained due to the analysis of many rock samples. The surface boundaries of the density bodies listed in Table 1 are directly taken from tectonic maps.

The deeper geometry was inspired by seismic findings (especially in areas of the molasse basins where industry data were available), maps of the sedimentary cover (Berthelsen et al., 1992), and other geological information (Lammerer and Weger, 1998; Lammerer, 1998). Only small adjustments were made during the process of optimisation of the density model in order to conform to the observed potential fields. The shallow geologic formations included in our model can be seen in Fig. 1.

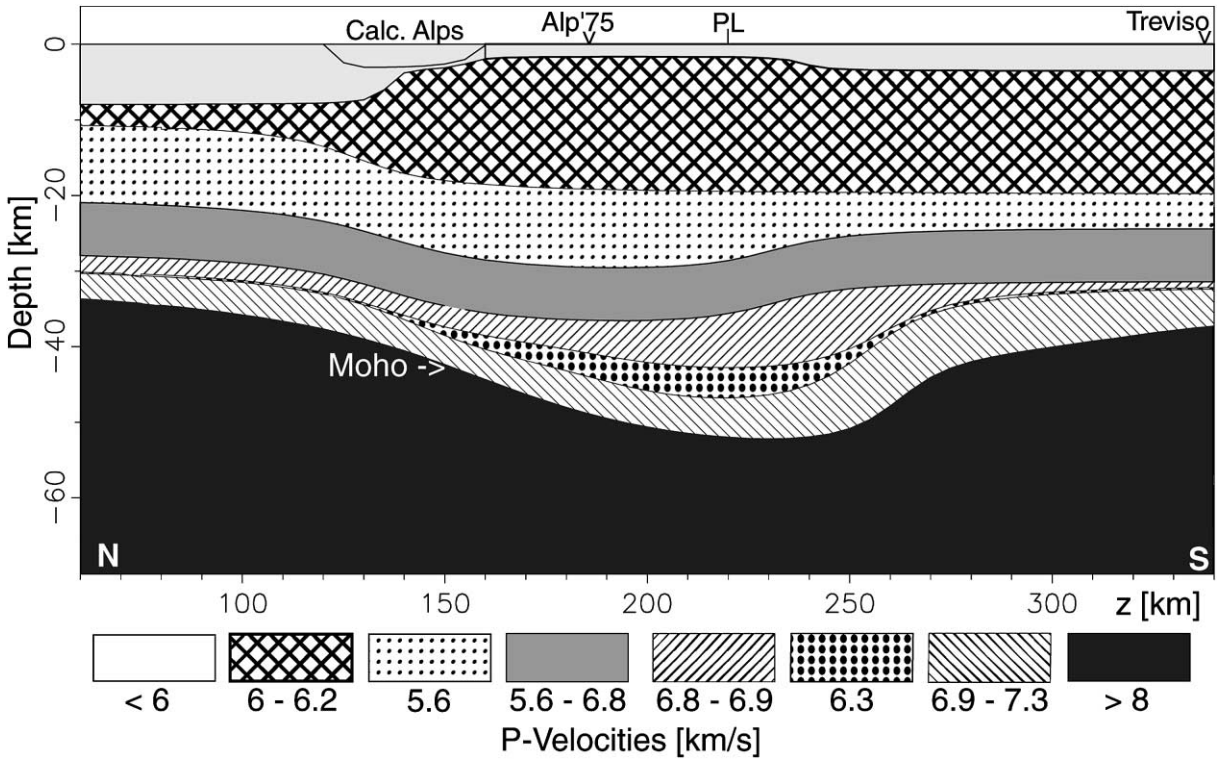

Fig. 4. The velocity model 'Eschen-38' (Miller et al., 1977) as completed by the TRANSALP Working Group (Bleibinhaus and TRANSALP Working Group, 2001). PL indicates the periadriatic lineament, which is not seen in the velocity profile.

The mapped modelled gravity which is caused by the model's density distribution down to a depth of approximately 10 km (Fig. 5a) highly correlates with the structures seen in the tectonic map of Fig. 1. This means that near surface geologic formations can be rather easily identified in the short wavelengths of the Bouguer anomaly: the contributions to the Bouguer gravity field of masses in the area of the northern molasse basin accounts for approx. -10×10^{-5} m/s^2, those of the Calcareous Alps up to $+25\times10^{-5}$ m/s^2, the Tauern window and nappe structures gives values between 0 and -20×10^{-5} m/s^2 (in the west), and to the south closely to the Periadriatic line some $+10\times10^{-5}$ m/s^2 in the Dolomites. The model effects of the sediments of the Po Basin are rather similar to those of the northern molasse basin.

These local gravity effects (Fig. 5b) were stripped off from the measured Bouguer gravity field and the obtained residual gravity field is similar to a smoothed observed Bouguer anomaly which can be calculated by lowpass filters. However, the overall low in the central part of the area broadened in the north–south direction and in the south the original high gravity became less pronounced than before the stripping

Table 1
The superficial formations presented in our model and the related density values (after Granser et al., 1989; Schöler, 1976)

Formation	Density (kg/m^3)
Northern molasse basin	2550
Alpine foreland molasse (Flysch)	2600
Penninic sediments	2700
Northern Calcareous Alps	2730
Austroalpine nappes	2740
Basement nappes	2550
Shist tauern	2700
Gneiss tauern	2550
Dolomites	2700–2750
Po-Plain	2400

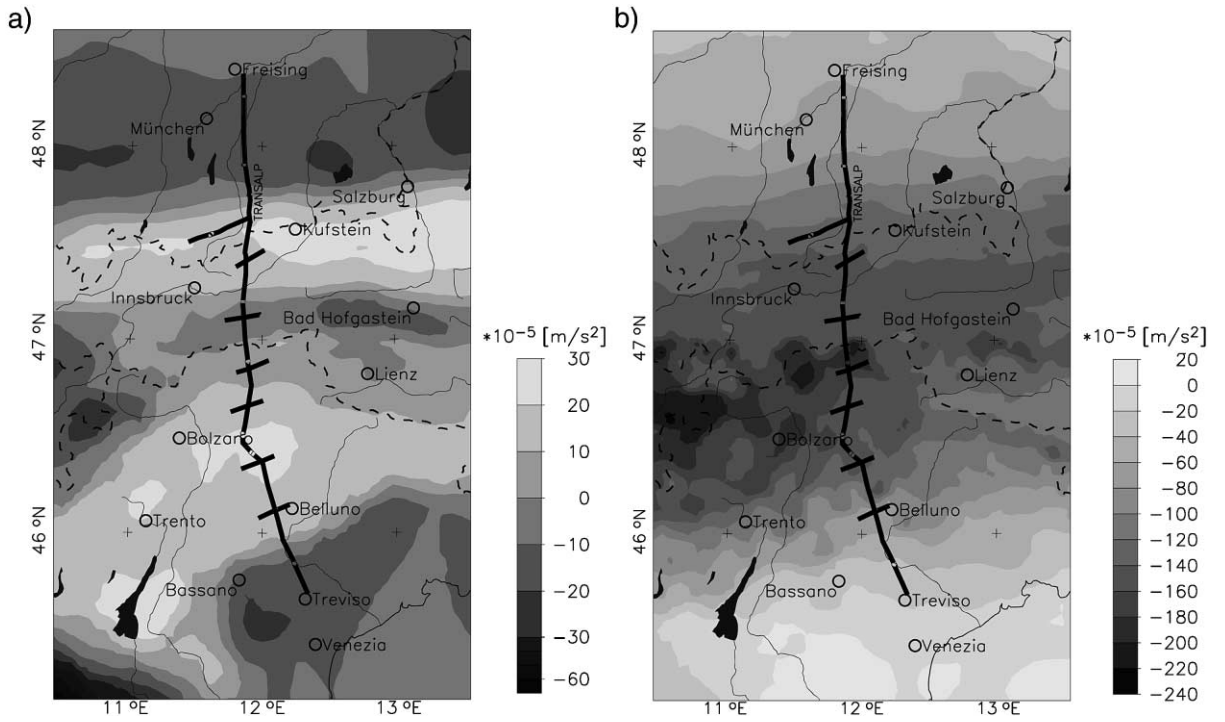

Fig. 5. Greyscale presentation of (a) the gravity effect of the upper 10 of the crust, and (b) the resulting stripped Bouguer anomaly.

procedure was applied to the Bouguer gravity. It is obvious that the stripped Bouguer anomaly reflects regional, long-wavelength anomalies only, which are caused by deep seated density inhomogeneities.

4.4. The lower crust

Those parts of the 3D model which contain the lower crust are constrained by the information of the velocity model 'Eschen-38' (after Miller et al., 1977; Fig. 4) which has been completed by the recent data of the TRANSALP project (Bleibinhaus, 2001; TRANSALP Working Group, 2001). The 'Eschen-38' model was modified by new findings of the TRANSALP Working Group, however, there still exist uncertainties between former interpretations and the new profile. One of these uncertainties concerns the identification of the Moho beneath the Tauern window in the axis of the Eastern Alps (Lueschen and TRANSALP Working Group, 2000). An explanation is the strong anisotropy in the upper crust and bands of crustal reflection patterns, which always make it difficult to obtain an exact image of the Moho in this area. The combined vibroseis/explosives seismic surveys are able to image the Moho boundary in the northern and southern edge. Also the dip in the direction of the Alpine axis is well constrained. But below the Alpine axis, and more to the south the deeper parts of the lithosphere are not resolved. Particularly, the interfingering structures which are parts of European and Adriatic plate are not well observed in the seismic sections (TRANSALP Working Group, personal communication). Towards this end, there is also a lack of firm information on the velocity structure which would be necessary to constrain the density structure. This was the main reason to design the density model mostly on top of the 'Eschen-38' interpretation (Fig. 4). Two noticeable observations have to be mentioned: (1) aside of the continuous crust–mantle boundary there lies a zone of inversion of seismic velocities at 10 and 20 km depth. In this area the P-velocity values decrease from 6.2 to 5.6 km/s, and (2) additionally a second zone of an inverse velocity gradient can be found in the area of the crustal root. Some 5 km above the Moho interface a body with an extension of about 100 km in

Table 2
Density values for the model, as calculated from seismic velocities and *after Suhadolc et al. (1990)

Formation	Density (kg/m^3)	Velocity (km/s)
Upper crust	2750–2850	6000–6200
Middle crust	2700–2750	5600–6200
Lower crust	2950–3150	6800–7300
Inversion zone	3000	6300
Lithospheric mantle	3360–3375	> 8000
Upper asthenospheric mantle*	3350	

north–south direction is visible, where P-Velocity values decrease from 6.9 to 6.3 km/s.

In order to calculate the densities of the 3D model this velocity model was interpolated in east–west direction and velocities were converted into densities by using velocity–density relationships after Sobolev and Babeyko (1994). Their approach is sensitive to local variations of the heat and pressure conditions in the lithosphere and provides rather 'realistic' densities. In Table 2 the rock density values are listed which were assigned to the model structures of the lower crust. Furthermore, this 3D model was modified by geometry information of the crust–mantle boundary following an interpretation of Giese and Buness (1992). Constraining the lithosphere–asthenosphere model boundary the velocity model of Suhadolc et al. (1990) was adopted. Regarding the lithosphere–asthenosphere boundary two models exist (Suhadolc et al., 1990; Babuska et al., 1990). As discussed in Kissling (1993) the two models differ in the geometry and in the values of lithospheric thickness. We have adopted the model of Suhadolc et al. (1990), as it seems to be the more reliable (Kissling, 1993). We have to emphasize that for Bouguer gravity modelling the influence of these particular models is not very significant, due to the long wavelengths involved and the low density contrast at the lithosphere–asthenosphere boundary (20 kg/m^3). Surprisingly, the influence on the terrain corrected geoid is not neglectable.

In the course of interactive model matching the initial 3D density model has been modified and adjusted to the Bouguer anomaly. From north to south we define three domains of each crustal layer: the northern Pre-Alps, the central Eastern Alps, and the Southern Alps, forming the European plate, the melange of European and Adriatic plate, and the Adriatic plate, respectively. Generally we obtained slightly lower density values for the Adriatic crust than for the European crust. The central region with the melange of Adriatic and European crust and high compression is generally characterized by relatively high densities. However, domains of extreme density lows are located at the top of the central Tauern Window and in the area of the crustal root in the seismic inversion zone.

4.5. The optimised 3D model

Fig. 6a illustrates the optimised density model along the TRANSALP transect from the northern Pre-, through the central Eastern and to the Southern Alps. In Fig. 6b the Moho map is shown as it results from the 3D modelling. The main difference between the gravity Moho, defined on density, in respect to the seismic Moho, defined on velocity, is, that the Moho trend is less smooth in the transition zone between the European and Adriatic crust. The depth of the Moho boundary is increasing steeper to the Adriatic domain and lies in the southern part significantly higher than in the velocity model.

5. Gravity inversion of the crust–mantle boundary

Because of the uncertainties in the geometrical structure of the lower crustal model from the seismic profiling, we also investigated the Moho undulations by the method of gravity inversion. The good constraints developed for the upper crustal model give an excellent means to free the observed Bouguer field from the contribution of the upper 10 km of the crust, and to use the modified field for the inversion.

Fig. 6. Presentations of the 3D density model. (a) The vertical cross-section presents a section from Freising to Treviso along the TRANSALP-Traverse. Dashed lines in the model represent the geometry of the velocity model 'Eschen-38' (Fig. 4)). For density values refer to Tables 1and 2. The conjunction with Alp'75 is in the central Tauern window. Profile kilometre 0–120 present the alpine foreland, 100–200 the Eastern Alps, 200–280 the Southern Alps and 280-end the alpine hinterland. The uplifted formations of the Tauern window are shown between 160 and 190 km on the profile. (b) The greyscaled Moho map is similar to Giese and Buness (1992), slightly modified during the course of optimisation of the model.

a)

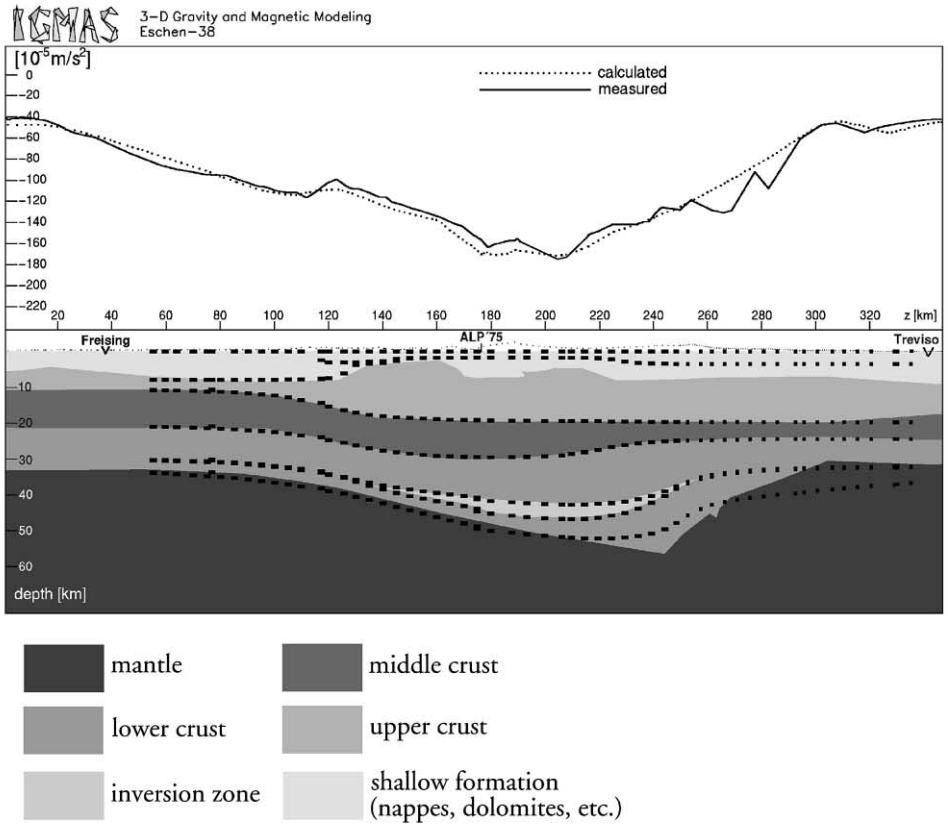
3–D Gravity and Magnetic Modeling
Eschen–38
[10⁻⁵m/s²]
calculated
measured
z [km]
Freising
ALP 75
Treviso
depth [km]
mantle
middle crust
lower crust
upper crust
inversion zone
shallow formation
(nappes, dolomites, etc.)

b)

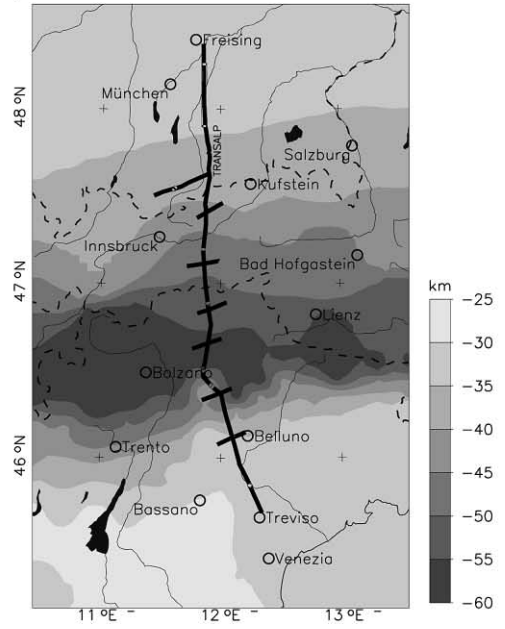
Freising
München
Salzburg
Kufstein
Innsbruck
Bad Hofgastein
Lienz
Bolzano
Belluno
Trento
Bassano
Treviso
Venezia
TRANSALP
km
48 °N
47 °N
46 °N
11 °E
12 °E
13 °E

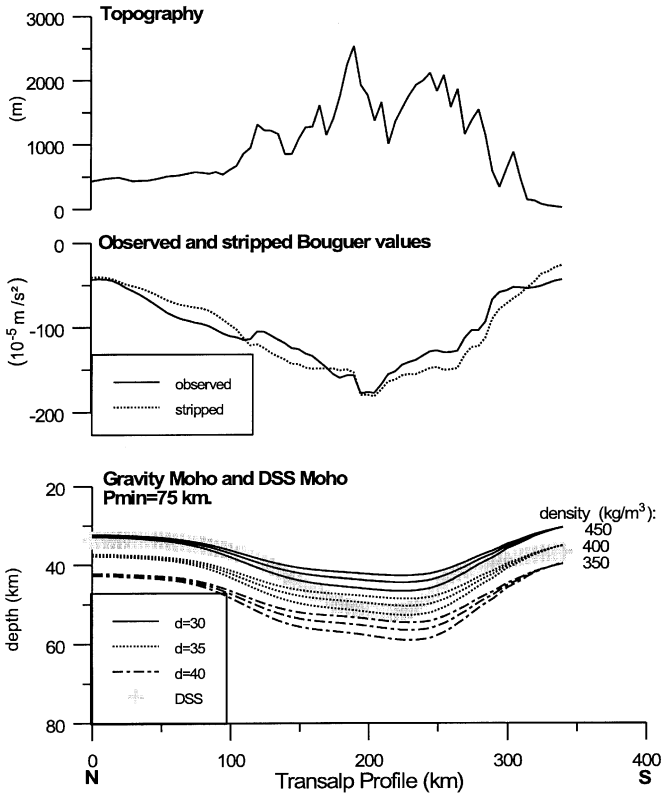

Fig. 7. Different solutions for the Moho depth along the TRANSALP-profile by gravity inversion. In the lower part the solutions of the inversion with different parameters together with the Moho depth from the velocity model 'Eschen-38' (dots) is presented. Pmin indicates the cut-off wavelengths of the cosine taper. Above the related observed Bouguer gravity and the stripped Bouguer gravity are shown. The upper part shows the topography along the profile.

The residual field (Fig. 5b) is subsequently low-pass filtered, according to the general observation that the contributions from the deeper layers affect increasingly lower spatial frequencies. We have estimated the cut off period by applying the method of Russo and Speed (1994) and Cianciara and Marcak (1976). The spectral analysis of the Bouguer field results in two main sources, first at a depth of 7 km, second one at a depth of 54 km. For the Moho inversion we chose a cosine taper filter with a cut-off wavelength of 75 km. These values are in the range of previous studies (e.g. Granser, 1989). With the above mentioned criteria this presumption shall be an adequate value in order to separate the Moho contributions from those of the middle to upper crust. The gravity inversion was made by an iterative method that alternates downward continuation with forward modelling. The crust–mantle boundary is modelled as an undulating surface that defines a density contrast (drho) and is set at a reference depth (*d*). The method has been already tested and successfully applied to different areas (Braitenberg et al., 1997, 2000; Braitenberg and Zadro, 1999). In the present study an improvement has been introduced regarding the direct modelling, which is now accomplished by a method of a stack of horizontal slices (Blakely, 1996) approximating the crustal roots, that replaces the discretisation with right rectangular prisms. The new method allows a substantial reduction of computation time, with an improvement in the approximation of the structures to be modelled. For the purpose of increased spectral resolution and in order to have a buffer zone for the border effects, the gravity field is extrapolated to all sides by 150 km, the resolution of the grid being 5×5 km.

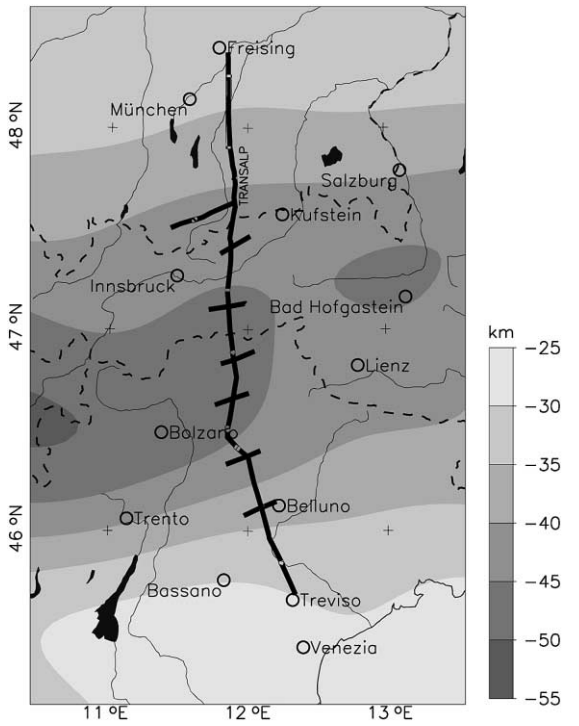

Fig. 8. Greyscale map of the Moho obtained from gravity inversion. The parameters used here are a reference Moho depth of 30 km with a density contrast of 350 kg/m^3.

The seismic Moho depths found along the TRANSALP profile, where available, are used as constraints for the solution. The solution is calculated for different couples of the reference depth (d) and density contrast (drho), that are allowed to attain the values 30, 35, 40 km and 350, 400, 450 kg/m^3, respectively. The number of iterations is fixed to three, as further iterations do not bring considerable improvement to the solution. In Fig. 7 the Moho solutions for different reference depths and density contrasts are graphed together with the Moho depths proposed from the TRANSALP velocity model. According to the part of the profile that is considered, a reference depth of 30 or 35 km, with a density contrast of 350 kg/m^3 gives the best match between the gravity and the seismic Moho. In the northern part the solution is best for the reference depth 30 km, in the southern part a reference depth of 35 km is preferable. We propose the solution of a reference depth of 30 km, as the agreement is better on a longer segment of the profile. Generally, the fitting is best in the northern part of the profile (Fig. 7). In the central part the gravity Moho lies shallower, which could be explained by the existence of mid-crustal reflections which disturb the inversion solution. In the southern part the gravity Moho is slightly shallower than what predicted from seismic profiling. This conforms though to the result obtained in the 3D forward modelling. The entire solution for the gravity Moho is shown in Fig. 8.

In comparison with the Moho that was conceived by 3D forward modelling it is obvious, that both methods essentially lead to very similar results. The gross features of the Moho undulations are in good agreement for both depths and geometry of density domains. The disparities are found in the area of Lienz, where according to gravity inversion, the Moho should be higher than predicted from the seismic model. Towards the Adriatic sea the inversion gives a slightly higher Moho, an area where no seismic lines are available and the seismic Moho model shows a lack of data, so that the Moho was interpolated for the course of forward modelling.

6. Discussion and conclusion

In this study we present a detailed model of lithospheric density in a 200-km-wide strip centred on the TRANSALP profile. The density model is constrained by nearly all available information which were deduced from seismic profiling, geology and tectonic investigations, conducted in the Eastern Alps. Similar to previous papers (e.g. Schöler, 1976; Granser et al., 1989) we figured out that the observed gravity is always caused by two main source depths. One, which is in the upper 10 km, is clearly connected with the obvious near-surface tectonic regime. The second source level is detected in the depth of the density contrast at the crust–mantle boundary or even deeper.

The uppermost 10 km of the model are well constrained by both observations from geology and seismic. In contrast to previous models (e.g. Makris, 1971; Cassinis et al., 1997) which had to dispose of rather generalized upper crustal structures, actually a more detailed imaging of near-surface structures is possible. There is a strong need for this detailed view because it leads to a better insight into the processes that built these geological structures and

their evolution in the Eastern Alps. This is why these structures have to be regarded and modelled as precise as possible. In the central part the density distribution of the upper crust is clearly related to uplift in this part, and reflects the kinematic evolution of the Tauern window. The small scaled structures cause gravity anomalies that superpose and interfere with the regional gravity field caused by the Moho interface. Therefore, it is impossible to separate the small and long wavelengths of the gravity field in such complex environment by a simple low-pass filtering. Forward modelling under constraining conditions seems to be the only possibility to eliminate gravity effects of near-surface structures with the consequence that a regional (deeper) field can be calculated on the base of constrained information. This kind of regional field eases the construction of deeper located density structures.

Aside of the 'gravity stripping method' two other methods have been used here in this study to investigate lower crust and upper mantle density distributions, the first was an interactive 3D forward model matching. In this, a starting model was constructed on base of the seismic velocity distribution of both the TRANSALP velocity model and the Moho model of Giese and Buness (1992) which was stepwise interactively modified, and the second was gravity inversion. The gravity inversion is anchored by the Moho depths found along the TRANSALP profile. The inversion procedure gives a detailed model of the Moho that is independent from the pre-existing seismic velocity model. It is of value that uncertainties, if present in the velocity model, are not propagated into the density model. Essentially, the two methods agree in the resulting Moho.

Important features of the Moho are the crustal roots along the central part of the Alpine arch, that achieves a depth of 55 km. In the southwest a shallowing of the Moho is found that coincides with the gravity high of the Vicenza area. Moho depth here is significantly less than in the velocity model. The deepening of the Moho towards the central part of the Alps is relatively steeper in the Adriatic domain than in the Alpine domain, indicating an asymmetry with respect to the Alpine Arch. To the North of the Alps the two models agree to a gradual shallowing of the Moho depth to 30 km.

The model gravity that matched the Bouguer field in the entire are is given in Fig. 9a, and a comparison with the observed field in Fig. 3b can prove the satisfying coincidence between the two fields. The residual field (Fig. 9b) contains only local features.

The gravity effect of the upper 10 km masses amounts to 30×10^{-5} m/s^2. From east to west the Bouguer gravity field is strongly caused by tectonically uplifted structures of the Tauern window and erosion of the Helvetic and Penninic nappes. This is clearly seen if the gravity effect of the upper 10 km model section is compared with the tectonic map at the surface (Figs. 1 and 5a). The main influence on the Bouguer anomaly and the terrain corrected geoidal undulations is given by the density contrast of the crust–mantle–boundary. Therefore it is driven by the inherent density contrast of some 350 kg/m^3. This density contrast corresponds with the findings of previous studies (e.g. Makris, 1971; Holliger and Kissling, 1992; Cassinis et al., 1997; Dal Moro et al., 1998). The fitting between modelled (Fig. 9c) and observed terrain corrected geoidal undulations (Fig. 3c) is not as good, as a general misfit of around 70 m was found. The map of the residual geoidal field (Fig. 9d) reveals two major features. One is the general shift of about 70 m between the level of the observed and the modelled field. In addition a north–south trending linear misfit of long wavelength is visible. Probably this misfit is linked with a density inhomogeneity in subcrustal or sub lithospheric levels. Even density variations in the deep mantle could be the source. Tomographic studies point also to subcrustal inhomogeneities (Spakman, 1990; Kummerow et al., 2000), which support this hypothesis. However, the identification of those structures was not subject to this study here. Both models seem to indicate a slightly higher crust–mantle–boundary in the Adriatic area than expected from the seismic profiling. The main structural changes are orientated north–south, but especially in the upper crust east–west oriented features have to be

Fig. 9. Greyscale maps of the results of 3D density modelling. Here the (a) modelled Bouguer anomaly, the (b) misfits between the modelled and observed Bouguer anomaly, (c) the modelled terrain corrected geoidal undulations, and (d) the misfits for the last are presented.

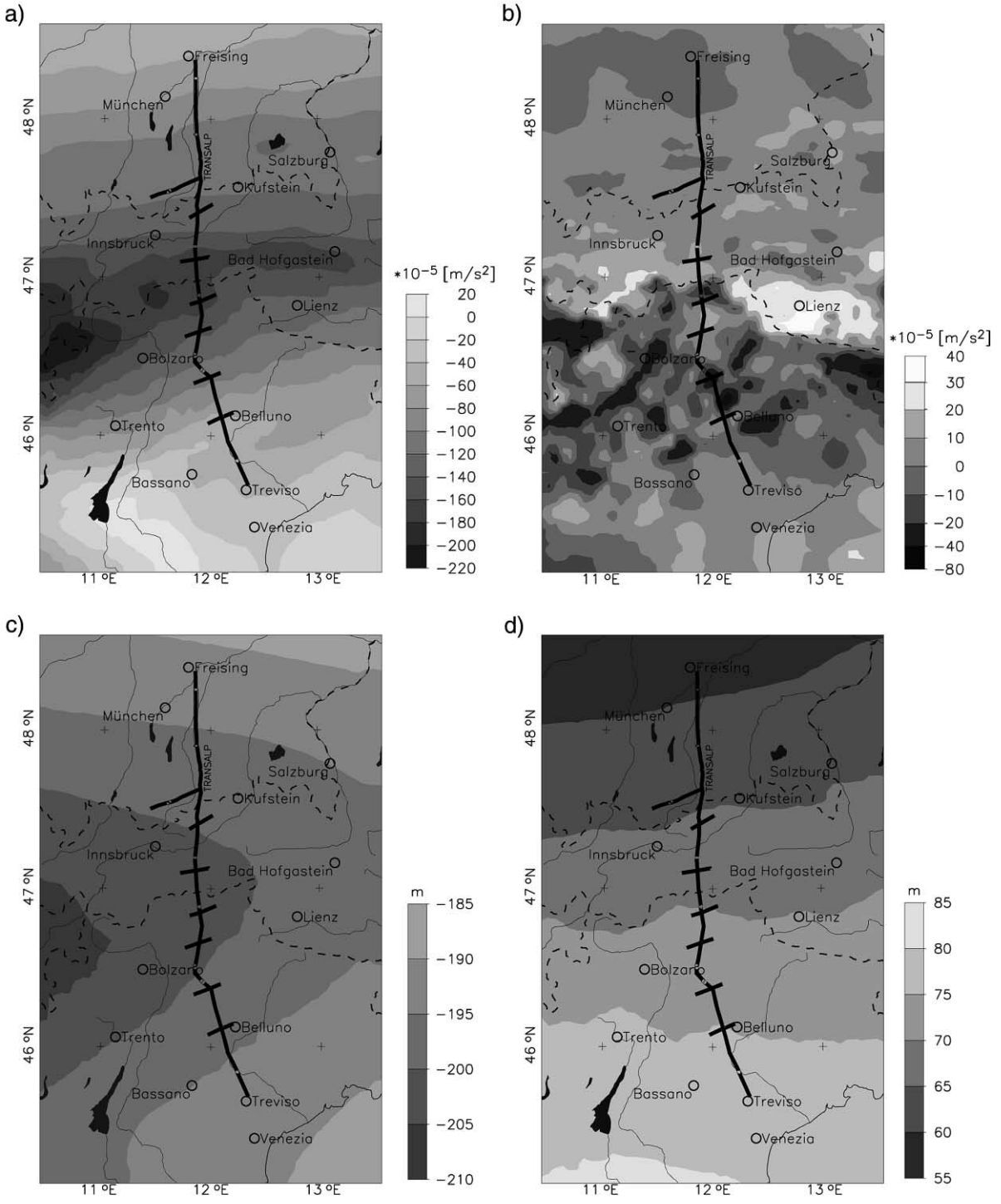
a)
b)
c)
d)
Freising
München
Salzburg
Kufstein
Innsbruck
Bad Hofgastein
Lienz
Bolzano
Belluno
Trento
Bassano
Treviso
Venezia
TRANSALP
48 °N
47 °N
46 °N
11 °E
12 °E
13 °E
*10−5 [m/s2]
20
0
−20
−40
−60
−80
−100
−120
−140
−160
−180
−200
−220
40
30
20
10
0
−10
−20
−40
−80
m
−185
−190
−195
−200
−205
−210
85
80
75
70
65
60
55

considered. Further improvement would consider a more detailed model and more constraining information from the seismic investigations.

To understand the collision process of the Adriatic and the European plate by investigating the shape of the Moho interface remains one of the major key problems. As various seismic experiments differ in their structural results, the presented gravity modelling can help to minimise existing uncertainties and help to extrapolate information from seismic studies which normally exist along seismic profiles only.

The Alps formed by collision of the composite Austroalpine — South Alpine promontory of the Adriatic microplate and the European plate after the southward to southeastward subduction of an intervening strip of oceanic lithosphere. In high structural levels of the Alps three major, non-coaxial stages of contraction are recorded (Pfiffner, 1992; Froitzheim et al., 1994; Eisbacher and Brandner, 1996; Kley and Eisbacher, 1999). The first stage, of middle to late Cretaceous age, involved the west- to northwest-directed stacking of Austroalpine crust within the Adriatic plate. The second stage with its climax in Eocene time led to the subduction of the South Penninic ocean, the formation of an ophiolitic suture, and the northerly to north–northeasterly emplacement of the internally deformed Austroalpine thrust complex over Penninic and Helvetic units of the European passive margin. These structures cause the short wavelength gravity field in the Eastern Central Alps (e.g. Tauern window) that is observable in the residual gravity and the new TRANSALP reflections as well (Lueschen and TRANSALP Working Group, 2001). A third stage of post-collisional thrusting affected both European and Adriatic basement units. However, three-dimensional complexities during the Alpine extension and contraction also prompted long-lived polyphase displacements along strike-slip fault such as the Periadriatic Line. A strong north–south asymmetry of Bouguer gravity was modelled here with soft horizontal gradients in the north and more pronounced ones in the south as a crustal response of collision.

A future combination of seismic, density and geological models will help to shed more light on this critical collision front and the understanding of the isostatic state of the Eastern Alps. From earlier investigations (e.g. Wagini et al., 1988; Götze et al., 1991) we know that the Eastern Alps are not isostatically balanced in the sense of simple Airy-Heiskanen isostasy. As our results show, other effects than simple topographic loading have to be regarded. Especially the calculation of subsurface loads caused by density distributions in the crust and upper mantle are important factors to interpret the isostatic state through depth and the isostatic anomalies in the sense of over- and under compensated Alpine and/or Adriatic microplate lithosphere. Our results show that also subcrustal density inhomogeneities have to be considered and playing an important role for the isostatic state of the Eastern Alps. Although the influence of subcrustal/sublithospheric domains on the Bouguer gravity field is small, it is not neglectable. Modelling of deep seated density inhomogeneities and the calculation of lithospheric rigidity by the aid of Vening–Meinesz models will help us to detect forces and conditions connected to processes which act on the Alpine mountain building and the motions of Adriatic and European plate.

Acknowledgements

Careful reviews by R. Cassinis and an anonymous reviewer helped us to improve the manuscript. We gratefully thank B. Meurers of the University of Vienna who provided the Austrian gravity data for our use and contributed to initial ideas. For obtaining gravity data of the Italian and German area we thank the Bureau Gravimetrique International (Toulouse) and the Institut für Geowissenschaftliche Gemeinschaftsaufgaben (Hannover), respectively. The authors express their gratitude to H. Gebrande, E. Lueschen and the other members of the TRANSALP Working Group for providing new results of the seismic investigations. We want to thank S. Schmidt, who provided software. The research is funded by the Deutsche Forschungsgemeinschaft (Go 380/19-1, 19-3), and by CNR grants 98.00159 and 97.00121 and MURST 60%, which is thankfully acknowledged.

References

Alpine Explosion Seismology Group, 1976. A lithospheric seismic profile along the axis of the Alps, 1975 — First Results. Reporter: Miller, H. Pure Appl. Geophys. 114, 1109–1130.

Babuska, V., Plomerova, J., Granet, M., 1990. The deep lithosphere

in the Alps: a model inferred from P residuals. Tectonophysics 176, 137–165.

Berthelsen, A., Burrolet, P., Dal Piaz, G.V., Franke, W., Trümpy, R., 1992. Tectonics. In: Blundell, D., Freeman, R., Mueller, St. (Eds.), A Continent Revealed: The European Geotraverse. Cambridge University Press, New York.

Blakely, R.J., 1996. Potential Theory in Gravity and Magnetic Applications. Cambridge University Press, New York.

Bleibinhaus, F., TRANSALP Working Group, 2001. Velocity structure in the Eastern Alps along the TRANSALP profile. Geophys. Res. Abstr. 3, 620.

Braitenberg, C., Zadro, M., 1999. Iterative 3D gravity inversion with integration of seismologic data. Boll. Geof. Teor. Appl. 40 (3-4), 469–476.

Braitenberg, C., Pettenati, F., Zadro, M., 1997. Spectral and classical methods in the evaluation of Moho undulations from gravity data: the NE-Italian Alps and isostasy. J. Geodyn. 23, 5–22.

Braitenberg, C., Zadro, M., Fang, J., Wang, Y., Hsu, H.T., 2000. The gravity and isostatic Moho undulations in Qinghai-Tibet plateau. J. Geodyn. 30 (5), 489–505.

Breunig, M., Cremers, A.B., Götze, H.-J., Schmidt, S., Seidemann, R., Shumilov, S., Siehl, A., 2000. Geological mapping based on 3D models using an interoperable GIS Geo-Information-Systems. J. Spatial Inf. Decision Making 13, 12–18.

Cassinis, R., Federici, F., Galmozzi, A., Scarascia, S., 1997. A 3D gravity model of crustal structure in the Central-Eastern Alpine sector. Ann. Geofis., XL 5, 1095–1107.

Christensen, N.I., Mooney, W.D., 1995. Seismic velocity structure and compositions of the continental crust: a global view. J. Geophys. Res. 100 (B7), 9761–9788.

Cianciara, B., Marcak, H., 1976. Interpretation of gravity anomalies by means of local power spectra. Geophys. Prospect. 24, 273–286.

Dal Moro, G., Braitenberg, C., Zadro, M., 1998. Geometry and mechanical crustal properties in NE Italy based on seismic and gravity data. Boll. Geof. Teor. Appl. 39, 37–46.

Deichmann, N., Ansorge, A., Mueller, St., 1986. Crustal structure of the southern Alps beneath the intersection with the European Geotraverse. Tectonophysics 126, 57–83.

Eisbacher, G.H., Brandner, R., 1996. Superposed fold-thrust structures and high-angle faults, northwestern Calcareous Alps, Austria. Eclogae Geol. Helv. 89, 553–571.

Frisch, W., 1979. Tectonic progradation and plate tectonic evolution of the Alps. Tectonics 60, 11–15.

Froitzheim, N., Schmid, S.M., Conti, P., 1994. Repeated change from crustal shortening to orogen-parallel extension in the Austroalpine nappes of Graubünden. Eclogae Geol. Helv. 87, 559–621.

Giese, P., Buness, H., 1992. Moho depth. In: Blundell, D., Freeman, R., Mueller, St. (Eds.), A Continent Revealed: The European Geotraverse. Cambridge University Press, New York.

Giese, P., Nicolich, R., Reutter, K.-J., 1982. Explosion crustal seismic studies in the Alpine–Mediterranean region and their implications to tectonic processes. In: Berckhemer, H., Hsü, K.J. (Eds.), Alpine–Mediterranean Geodynamics. AGU Series vol. 7, 347–376.

Götze, H.-J., 1984. Über den Einsatz interaktiver Computergraphik im Rahmen 3-dimensionaler Interpretationstechniken in Gravimetrie und Magnetik. Habil. Schrift, TU Clausthal.

Götze, H.-J., Lahmeyer, B., 1988. Application of three-dimensional interactive modelling in gravity and magnetics. Geophysics 53 (8), 1096–1108.

Götze, H.-J., Meurers, B., Schmidt, S., Steinhauser, P., 1991. On the isostatic state of the Eastern Alps and the Central Andes — a statistical comparison. In: Harmon, R.S., Rapela, C.W. (Eds.), Andean Magmatism and its Tectonic Setting. GSA Special Paper 265, 279–290.

Granser, H., Meurers, B., Steinhauser, P., 1989. Apparent density mapping and 3D gravity inversion in the Eastern Alps. Geophys. Prospect. 37, 279–292.

Holliger, K., Kissling, E., 1992. Gravity interpretation of a unified 2-D acoustic image of the central Alpine collision zone. Geophys. J. Int. 111, 213–225.

Italian Explosion Seismology Group, 1978. Preliminary interpretation of the profile HD across the eastern Alps. Boll. Teor. Appl. 20/79, 287–301.

Italian Explosion Seismology Group and Institute of Geophysics and ETH Zurich, 1981. Crust and upper mantle structures in the Southern Alps from deep seismic sounding (1977-8) and surface wave dispersion analysis. Boll. Teor. Appl. 3/92, 297–330.

Kennett, B.L.N., Engdahl, E.R., 1991. Traveltimes for global earthquake location and phase identification. Geophys. J. Int. 105, 429–465.

Kirchner, A., 1997. 3D-Dichtemodellierung zur Anpassung des Schwere-und Schwerepotentialfeldes der Zentralen Anden. Berliner Geowissenschaftliche Abhandlungen, B 25. Selbstverlag Fachbereich Geowissenschaften, FU Berlin.

Kissling, E., 1993. Deep structures of the Alps — what do we really know?. Phys. Earth Planet. Inter. 79, 87–112.

Kley, J., Eisbacher, G.H., 1999. How Alpine or Himalayan are the Central Andes? Int. J. Earth Sci. 88, 175–189.

Klingelé, E., Lahmeyer, B., Marson, I., Schwarz, G., 1990. A 2-D gravity model of the seismic refraction profile of the EGT Southern segment. In: Freeman, R., Mueller, St. (Eds.), Proceedings of the Sixth Workshop on the European Geotraverse (EGT) Project. European Science Foundation, Strasbourg, pp. 271–278.

Kummerow, J., Lippitsch, R., Kind, R., Kissling, E., TRANSALP Working GROUP, 2000. Seismic structure in the eastern Alps from teleseismic receiver functions. Abstract for Second International TRANSALP-Colloquium, Munich.

La Fehr, T.R., 1991. Standardization in gravity reduction. Geophysics 56 (8), 1170–1178.

Lammerer, B., 1998. Geologisches Profil durch die Ostalpen im Bereich der TRANSALP. http://www.iaag.geo.uni-muenchen.de/asa/asa_transalp.html.

Lammerer, B., Weger, M., 1998. Footwall uplift in an orogenic wedge: the Tauern window in the Eastern Alps of Europe. Tectonophysics 285 (3–4), 213–230.

Lelgemann, D., Kuckuck, H., 1992. Geoid undulations and horizontal gravity disturbance components. In: Blundell, D., Freeman, R., Mueller, St. (Eds.), A Continent Revealed: The European Geotraverse. Cambridge University Press, New York.

Lueschen, E., TRANSALP Working Group, 2000. TRANSALP — new deep seismic images of the Eastern Alps. Eos Trans. AGU 81 (48) Fall Meet. Suppl..

Makris, J., 1971. Aufbau der Kruste in den Ostalpen aus Schweremessungen und die Ergebnisse der Refraktionsseismik. Hamburger Geophysikalische Einzelschriften, Heft 15. Selbstverlag der Geophysikalischen Institute, Hamburg.

Miller, H., Gebrande, H., Schmedes, E., 1977. Ein verbessertes Strukturmodell für die Ostalpen, abgeleitet aus refraktionsseismischen Daten unter Berücksichtigung des Alpen-Längsprofils. Geol. Rundschau 98, 77–93.

Miller, H., Mueller, St., Perrier, G., 1982. Structure and dynamics of the Alps: a geophysical inventory. In: Berckhemer, H., Hsü, K. (Eds.), Alpine–Mediterranean Geodynamics. Am. Geophys. Union, Geodyn. Ser. 7, 175–204.

Mueller, St., Talwani, M., 1971. A crustal section across the eastern Alps based on gravity and seismic refraction data. Pure Appl. Geophys. 85, 226–239.

Müller, A., 1999. Ein EDV-orientiertes Verfahren zur Berechnung der topographischen Reduktion im Hochgebirge mit digitalen Geländemodellen am Beispiel der Zentralen Anden. Berliner Geowissenschaftliche Abhandlungen, B34, Selbstverlag Fachbereich Geowissenschaften, FU Berlin.

Pfiffner, A., 1992. Alpine Orogeny. In: Blundell, D., Freeman, R., Mueller, S. (Eds.), A Continent Revealed: the European Geotraverse. Cambridge University Press, Cambridge, pp. 180–190.

Pfiffner, O.A., Lehner, P., Heitzmann, P., Mueller, St., Steck, A. (Eds.), 1997. Deep Structure of the Swiss Alps. Results of NRP 20. Birkhäuser, Basel.

Rosner, M., 1994. Reinterpretation der Krustenstruktur der Ostalpen mittels strahlenseismischer 3D-Modellrechnung. Diplomarbeit, Univ. München.

Roure, F., Polino, R., Nicolich, R., 1990. Early Neogene deformations beneath the Po plain constraints on the post-collisional Alpine evolution. In: Coward, M.P., Dietrich, D., Park, R.G. (Eds.), Alpine Tectonics. Geol. Soc. Lond. Spec. Publ. 45, 309–321.

Russo, R.M., Speed, R.C., 1994. Spectral analysis of gravity anomalies and the architecture of tectonic wedging, NE Venezuela and Trinidad. Tectonics 13 (2), 613–622.

Sandwell, D.T., Smith, W.H.F., Smith, S.M., Small, C., 2000. Seafloor topography. http://topex.ucsd.edu/marine_topo/mar_topo.html.

Scarascia, S., Cassinis, R., 1997. Crustal structures in the central-eastern Alpine sector: a revision of the available DSS data. Tectonophysics 271, 157–188.

Schmidt, S., Götze, H.-J., 1998. Interactive visualization and modification of 3D models using GIS functions. Phys. Chem. Earth 23 (3), 289–296.

Schmidt, S., Götze, H.-J., 1999. Integration of data constraints and potential field modelling — an example from southern Lower Saxony, Germany. Phys. Chem. Earth (A) 24 (3), 191–196.

Schöler, W., 1976. Die Krustenstruktur der Ostalpen nach Ergebnissen gravimetrischer Untersuchungen unter besonderer Berücksichtigung der gemessenen Vertikalgradienten. Diss. TU Clausthal.

Schwendener, H., Mueller, St., 1990. A three-dimensional model of the crust and upper mantle along the Alpine part of the European Geotraverse (EGT). Tectonophysics 176, 193–214.

Sobolev, S., Babeyko, A., 1994. Modeling of mineralogical composition, density and elastic wave velocities in anhydrous magmatic rocks. Surv. Geophys. 15, 515–544.

Spakman, W., 1990. The structure of the lithosphere and mantle beneath the Alps as mapped by delay time tomography. The European geotraverse: integrative studies. Results from the Fifth Study Centre. European Science Foundation, Strasbourg.

Suhadolc, P., Panza, G.F., Mueller, S., 1990. Physical properties of the lithosphere–asthenosphere system in Europe. Tectonophysics 176, 123–135.

TRANSALP Working Group, 2001. European research project transects the Eastern Alps. Submitted for Publication.

US Geological Surveys, 2000. GTOPO30 — Global topographic data. http://edcdaac.usgs.gov/gtopo30/gtopo30.html.

Wagini, A., Steinhauser, P., Meurers, B., 1988. Isostatic residual gravity map of Austria. US Geological Survey Open File Report, pp. 87–402.

Yan, Q.Z., Mechie, J., 1989. A fine structural section through the crust and lower lithosphere along the axial region of the Alps. Geophys. J. 98, 465–488.